Enhancement of chlorophyll-a concentration south of Luzon Strait induced from bio-physical interaction during the PDO cold phase

Tseng Y.H.[1*] and Ho, C.R.[2]

[1]Ph.D. student, Department of Marine Environmental Informatics, National Taiwan Ocean University, Keelung, Taiwan

[2]Distinguished Professor, Department of Marine Environmental Informatics, National Taiwan Ocean University, Keelung, Taiwan

*21281001@email.ntou.edu.tw

Abstract *A region of high sea surface chlorophyll-a (Chl-a) concentration exists along the coast of northern Luzon Island, based on a 20-year average of MODIS-Aqua data. This target area lies west of the Kuroshio main route and east of the South China Sea (SCS) and serves as a transition of water interchanges. Monthly MODIS-Aqua level-3 data from August 2002 to August 2022 show that Chl-a concentrations in the target area are significantly higher during the Pacific Decadal Oscillation (PDO) cold phase (negative PDO index) compared to the PDO warm phase (positive PDO index), up to 0.4 mg m*$^{-3}$*. Meanwhile, the composite Kuroshio velocity during negative PDO indices indicates that the Kuroshio is accelerating south of the latitude of Luzon Island's northeastern tip (approximately 18°N) and decelerating north of 18°N. This state of current fields traps nutritious materials from the Cagayan River estuary, creating a favorable environment for Chl-a blooms. Furthermore, it prevents the intrusion of low-nutrient Kuroshio into the SCS through the southern Luzon Strait and the presence of high Chl-a concentrations longer than the period when the PDO index is positive.*

Keywords: chlorophyll-a, Pacific Decadal Oscillation, Luzon Island, Kuroshio, MODIS

Introduction

The Pacific Decadal Oscillation (PDO) is a long-lived pattern of Pacific climatic variability that has considerable impacts on surface chlorophyll-a (Chl-a) concentrations in the Pacific Ocean (Duteil et al., 2018; Lin et al., 2014; Mantua & Hare, 2002). A positive PDO phase is associated with a general decrease in Chl-a concentration in the tropical Pacific Ocean (Duteil et al., 2018). The PDO modulates decadal oscillations in Chl-a in the Kuroshio Extension region of the western Pacific Ocean (Lin et al., 2014). Chl-a exhibits correlated patterns with physical factors such as the PDO and North Pacific Gyre Oscillations (NPGO) in the Pacific Ocean (Hou et al., 2016). Climate reconstructions based on tree rings and corals reveal that PDO oscillations date back at least to A.D.1600 (Biondi et al., 2001) and interdecadal changes in the Pacific climate caused by the PDO have widespread impacts on marine ecosystems, including many North Pacific fisheries (Mantua & Hare, 2002). Therefore, the PDO plays an essential role in the decadal-scale variability of Chl-a concentrations in the Pacific Ocean, with a positive PDO phase generally associated with lower Chl-a levels in the tropics and modulation of Chl-a oscillations in the western Pacific.

Literature Review

The Chl-a concentration in the coastal region north of Luzon Island (North Luzon Coast, NLC hereafter) is influenced by several factors. First, upwelling is a key cause of high Chl-a concentration by bringing nutrients-rich deeper waters to the surface to stimulate phytoplankton growth (Gao et al., 2021). One of the common upwelling triggers is the Kuroshio interacting with the complex topography around Luzon Island. Second, the intrusion of the Kuroshio into the South China Sea (SCS) through the Luzon Strait contributes nutrients that enhance phytoplankton blooms in the NLC (Cabrera et al., 2015; Cordero-Bailey et al., 2021). Third, runoff providing terrestrial nutrients mainly from the Cagayan River on the north coast of Luzon Island can fertilize nearshore phytoplankton blooms, especially during the rainy season or the heavy typhoon-induced rainfall causing favorable current conditions (Zhao et al., 2013). Seasonally, the winter monsoon can drive enhanced mixing and upwelling, which sustains the winter phytoplankton blooms northwest of Luzon Island (Gao et al., 2021; Peñaflor et al., 2007; Shang et al., 2012).

The temperature range of 20–25°C is generally favorable for phytoplankton growth (Eppley, 1972; Grimaud et al., 2017; Rhee & Gotham, 1981). Peñaflor et al. (2007) suggested that the deflection of a branch of Kuroshio penetrating into the Babuyan Channel (south of Babuyan Islands) near the mouth of the Cagayan River probably traps the majority of the river discharge within several kilometers of the NLC.

Data and Methodology

a. Geographic Data

The data of the topography that distinct ocean and land, ETOPO1 1 Arc-Minute Global Relief Model, are provided by the National Geophysical Data Center, National Oceanic and Atmospheric Administration (NOAA) downloaded from https://doi.org/10.7289/V5C8276M (Amante & Eakins, 2009). Its global grid has a one-minute resolution. Additionally, the distribution of the river is important information to depict the source of nutrient outflow from the inland area to the NLC. We utilized ASTER Global Water Bodies Database V001 (https://doi.org/10.5067/ASTER/ASTWBD.001) to present the location of the Cagayan River in the northern Luzon Island. As shown in

Figure 1, the main river water source is indicated as the Cagayan River by the black streamline on the land.

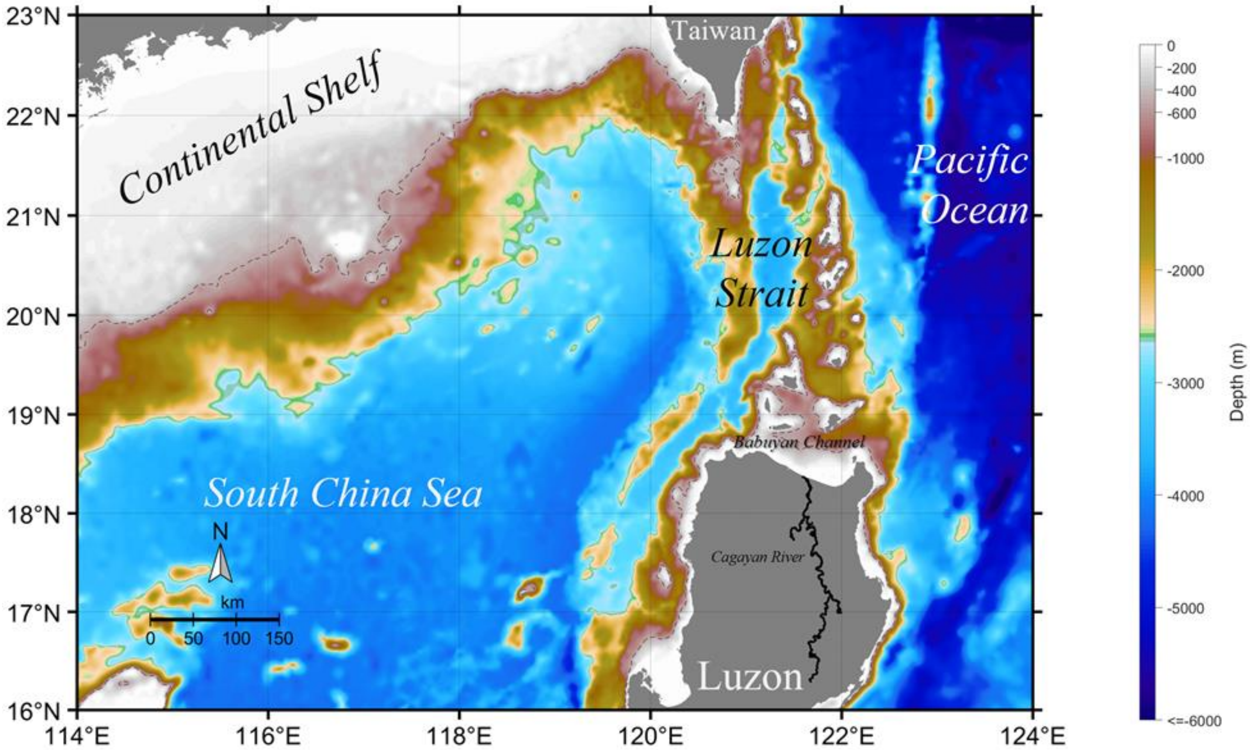

Figure 1: The study area near the Luzon Strait. The shading colors represent the depth of the ocean. The black streamline on Luzon Island denotes the Cagayan River. Dashed contours are at a depth of 500 meters.

b. Geostrophic current

The geostrophic current can be derived from the absolute dynamic topography (ADT) of the Copernicus Marine Environment Monitoring Service product (https://doi.org/10.48670/moi-00148, downloaded in September 2022) using geostrophic balance equations. The eastward component of the geostrophic current is $u = -\frac{g}{f}\frac{\partial \eta}{\partial y}$ and the northward component is $v = \frac{g}{f}\frac{\partial \eta}{\partial x}$, where η is ADT, g is the gravitational acceleration, and f is the Coriolis parameter (i.e., $f = 2\Omega \sin \theta$, where Ω is the angular velocity of the earth and θ is the latitude). The data comprise ADT data from 1993 to 2021, with a spatial resolution of 0.25° × 0.25° and a daily temporal resolution.

c. Chl-a

The monthly Level-3 (L3) Moderate Resolution Imaging Spectroradiometer (MODIS) Chl-*a* data from August 2002 to August 2022 used in this study is provided by the National Aeronautics and Space Administration–Goddard Space Flight Center (NASA–

GSFC) at their website (https://oceancolor.gsfc.nasa.gov/). The spatial resolution of MODIS data is 4 kilometers. However, there is missing data on them. The merged L3 chlorophyll data and the fully normalized remote sensing reflectance at 443, 551, and 555 nm provided by the GlobColour (http://globcolour.info) exhibit a more comprehensive view of the satellite observation. It combines the satellite ocean color data obtained from optical sensors, including SeaWiFS, MODIS, and MERIS (Maritorena et al., 2010), and has been developed, validated, and distributed by ACRI-ST, France. To compare the MODIS data and GlobColuor data, the correlation between them shows that they are highly correlated.

d. PDO index

Performing as a climate index in the Pacific basin, the PDO is often seen as a long-lived El Niño-like mode of climate variability (Deser et al., 2012). The PDO used in this study is provided by NOAA's National Centers for Environmental Information (NCEI) (https://www.ncei.noaa.gov/pub/data/cmb/ersst/v5/index/), which is based on NOAA ERSST V5.

e. Composite Method

The analysis used in this study is a composite method (Lin et al., 2022; Yan et al., 2022) to distinguish the difference in Chl-a between the negative and positive PDO phases. After identifying the time series of the PDO index from August 2002 to August 2022, composite analysis can combine the distribution of Chl-a during the negative PDO phase and the positive PDO phase, respectively. The validity of composite analysis can be inferred from the grid points that are statistically significant above a 90% confidence level.

Results and Discussion

By analyzing the Chl-a concentration obtained from MODIS-Aqua data, it can be seen that the average Chl-a concentration from 2002 to 2022 (Figure 2) is at a relatively high level in the coastal region of the Cagayan River's estuary. The average flow field of the Kuroshio also shows that the high Chl-a concentration is this coastal area is suppressed by the Kuroshio (Figure 2). To investigate whether the Chl-a concentration is affected by the PDO, we show the difference between the composite Chl-a concentration during the PDO negative and positive phases (Figure 3). This significant difference indicated that the average Chl-a concentrations was high in the negative PDO phase than in the positive PDO phase, up to 0.4 mg m^{-3}. Furthermore, the composite Kuroshio current field also demonstrates the impact of the PDO phase on Chl-a concentration. During the negative PDO phase, the Kuroshio east of Luzon Island exhibits a more pronounced northward flow velocity and intrudes further into the Luzon Strait in a northerly direction. During the positive PDO phase, the Kuroshio exhibits reduced northward flow velocity and intrudes further south into the Luzon Strait. This disparity in the Kuroshio intrusion position can be observed by comparing its behavior between the positive and negative PDO phases (Figure 4). The nutrient-poor Kuroshio flows southward upon intruding into the Luzon Strait, hence suppressing the growth of Chl-a in the northern coastal regions of Luzon Island.

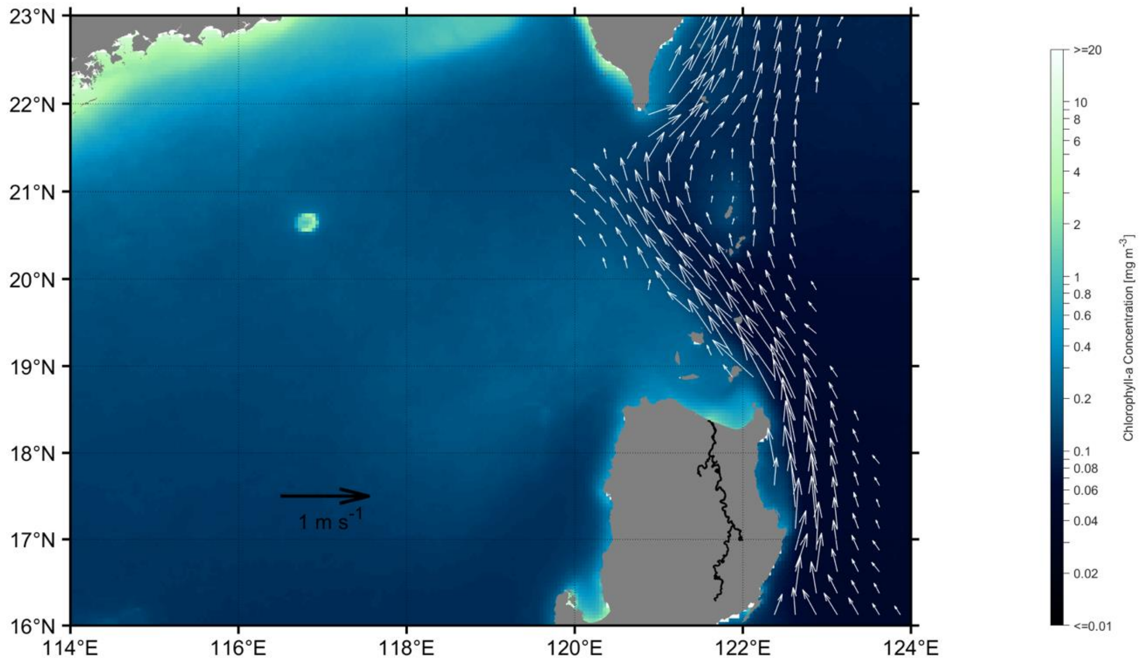

Figure 1: The mean state of MODIS Chl-a concentration near the region of the Luzon Strait from August 2002 to August 2022 (unit: mg m^{-3}). White vectors are the averaged geostrophic current of the Kuroshio from August 2002 to 2022 (unit: m s^{-1}).

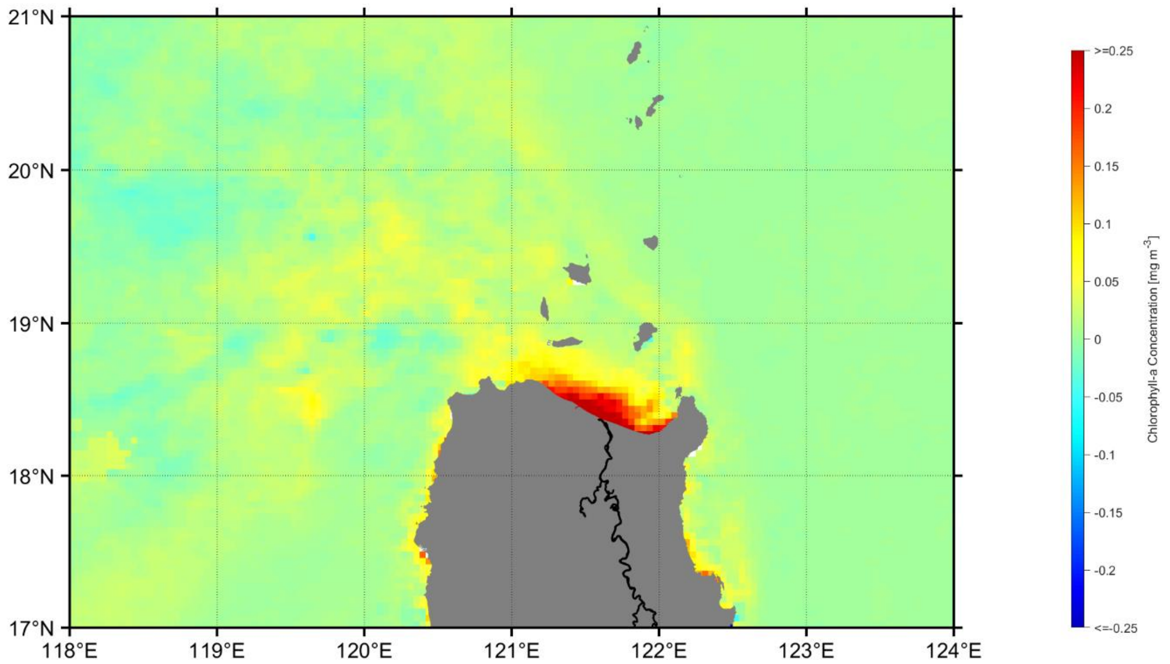

Figure 3: The composite Chl-a concentration difference between the negative PDO phase and the positive PDO phase from August 2002 to August 2022.

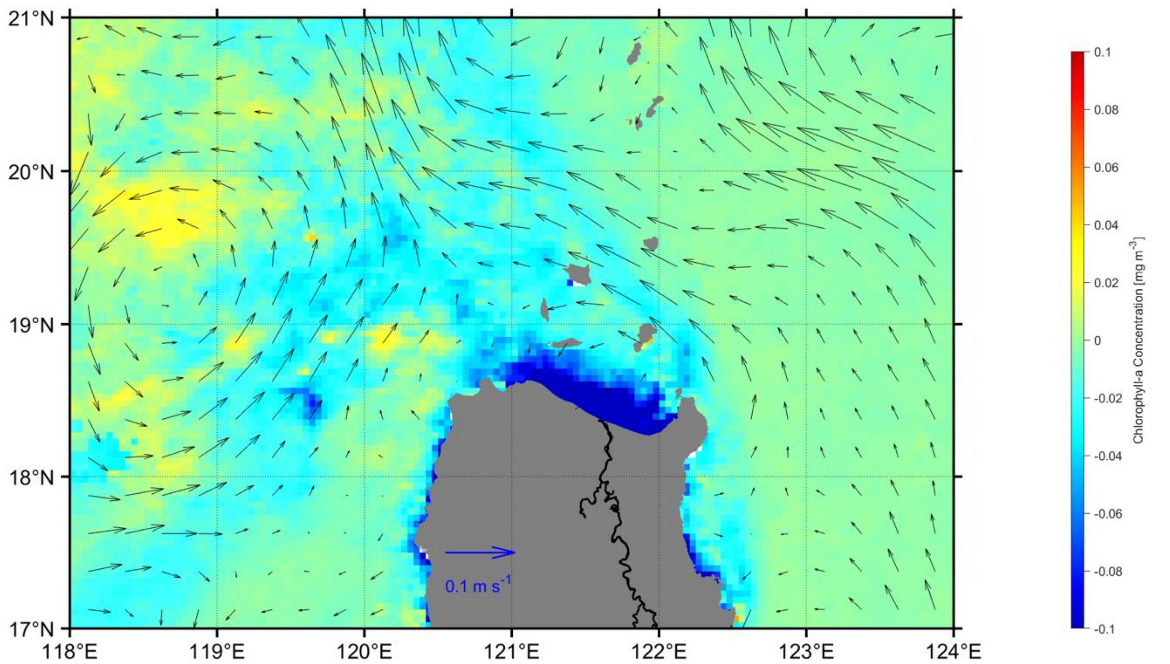

Figure 4: The difference of the geostrophic current fields near the northern Luzon Island between the positive and negative 3-month running mean PDO phases.

Conclusion and Recommendation

This study analyzed the Chl-a concentration on the northern coast of Luzon Island caused by the Cagayan River and its relationship with the Kuroshio intrusion into the Luzon Strait at different PDO phases. The results of this research can be summarized as follows: (1) When the Kuroshio during the negative PDO phase, it will be more northerly when it intrudes into the Luzon Strait; conversely, it will be more southerly. (2) Near the northern coast of Luzon Island, the Chl-a concentration will be more in the negative PDO phase. (3) The low-nutrient Kuroshio water may control the changes in Chl-a concentration on the northern coast of Luzon Island.

References

Amante, C., & Eakins, B. W. (2009). *ETOPO1 1 arc-minute global relief model: Procedures, data sources and analysis*. NOAA Technical Memorandum NESDIS NGDC-24. National Geophysical Data Center, NOAA. https://doi.org/10.7289/V5C8276M

Biondi, F., Gershunov, A., & Cayan, D. R. (2001). North Pacific Decadal Climate Variability since 1661. *Journal of Climate*, *14*(1), 5–10. https://doi.org/10.1175/1520-0442(2001)014

Cabrera, O., Villanoy, C., Alabia, I., & Gordon, A. (2015). Shifts in Chlorophyll *a* off Eastern Luzon, Philippines, Associated with the North Equatorial Current Bifurcation Latitude. *Oceanography*, *28*(4), 46–53. https://doi.org/10.5670/oceanog.2015.80

Cordero-Bailey, K., Bollozos, I. S. F., Palermo, J. D. H., Silvano, K. M., Escobar, M. T. L., Jacinto, G. S., Diego-McGlone, M. L. S., David, L. T., & Yñiguez, A. T. (2021). Characterizing the vertical phytoplankton distribution in the Philippine Sea off the northeastern coast of Luzon. *Estuarine, Coastal and Shelf Science*, *254*, 107322. https://doi.org/10.1016/j.ecss.2021.107322

Duteil, O., OChlies, A., & Böning, C. W. (2018). Pacific Decadal Oscillation and recent oxygen decline in the eastern tropical Pacific Ocean. *Biogeosciences*, *15*(23), 7111–7126. https://doi.org/10.5194/bg-2018-16

Eppley, R. W. (1972). Temperature and phytoplankton growth in the sea. *Fishery Bulletin*, **70**, 1063–1085.

Gao, H., Zhao, H., Han, G., & Dong, C. (2021). Spatio-Temporal Variations of Winter Phytoplankton Blooms Northwest of the Luzon Island in the South China Sea. *Frontiers in Marine Science*, *8*. https://doi.org/10.3389/fmars.2021.637499

Grimaud, G. M., Mairet, F., Sciandra, A., & Bernard, O. (2017). Modeling the temperature effect on the specific growth rate of phytoplankton: a review. *Reviews in Environmental Science and Bio/Technology*, *16*(4), 625-645. https://doi.org/10.1007/s11157-017-9443-0

Hou, X., Dong, Q., Hong, Y., Long, D., & Cui, Y. (2016). Coupled patterns between the surface chlorophyll-a and the physical factors in the Pacific Ocean. *In 2016 IEEE International Geoscience and Remote Sensing Symposium (IGARSS)*, 4581–4584. https://doi.org/10.1109/igarss.2016.7730195

Lin, P., Chai, F., Xue, H., & Xiu, P. (2014). Modulation of decadal oscillation on surface chlorophyll in the Kuroshio Extension. *Journal of Geophysical Research: Oceans*, *119*(1), 187–199. https://doi.org/10.1002/2013jc009359

Lin, J. Y., Zheng, Z. W., Zheng, Q., Wu, D. R., Gopalakrishnan, G., Ho, C. R., Pan, J., Lin, Y. C., & Xie, L. L. (2022). Satellite observed new mechanism of Kuroshio intrusion into the northern South China Sea. *International Journal of Applied Earth Observation and Geoinformation*, *115*, 103119. https://doi.org/10.1016/j.jag.2022.103119

Mantua, N. J., & Hare, S. R. (2002). The Pacific decadal oscillation. *Journal of Oceanography*, *58*(1), 35–44. https://doi.org/10.1023/a:1015820616384

Maritorena, S., d'Andon, O. H. F., Mangin, A., & Siegel, D. A. (2010). Merged satellite ocean color data products using a bio-optical model: Characteristics, benefits and issues. *Remote Sensing of Environment*, *114*(8), 1791-1804. https://doi.org/10.1016/j.rse.2010.04.002

Peñaflor, E. L., Villanoy, C. L., Liu, C. T., & David, L. T. (2007). Detection of monsoonal phytoplankton blooms in Luzon Strait with MODIS data. *Remote Sensing of Environment*, *109*(4), 443-450. https://doi.org/10.1016/j.rse.2007.01.019

Rhee, G. Y., & Gotham, I. J. (1981). The effect of environmental factors on phytoplankton growth: temperature and the interactions of temperature with nutrient limitation 1. *Limnology and Oceanography*, *26*(4), 635–648. https://doi.org/10.4319/lo.1981.26.4.0635

Shang, S., Li, L., Li, J., Li, Y., Lin, G., & Sun, J. (2012). Phytoplankton bloom during the northeast monsoon in the Luzon Strait bordering the Kuroshio. *Remote Sensing of Environment*, *124*, 38–48. https://doi.org/10.1016/j.rse.2012.04.022

Yan, X., Kang, D., Pang, C., Zhang, L., & Liu, H. (2022). Energetics analysis of the eddy–Kuroshio interaction east of Taiwan. *Journal of Physical Oceanography*, *52*(4), 647–664. https://doi.org/10.1175/JPO-D-21-0198.1

Zhao, H., Han, G., Zhang, S., & Wang, D. (2013). Two phytoplankton blooms near Luzon Strait generated by lingering Typhoon Parma. *Journal of Geophysical Research: Biogeosciences*, *118*(2), 412–421. https://doi.org/10.1002/jgrg.20041